



TITLE:

Analysis of subthreshold photo-leakage current in ZnO thin-film transistors using indium-ion implantation

AUTHOR(S):

Kamada, Yudai; Fujita, Shizuo; Hiramatsu, Takahiro; Matsuda, Tokiyoshi; Furuta, Mamoru; Hirao, Takashi

CITATION:

Kamada, Yudai ...[et al]. Analysis of subthreshold photo-leakage current in ZnO thin-film transistors using indium-ion implantation. Solid-State Electronics 2010, 54(11): 1392-1397

ISSUE DATE:

2010-11

URL:

<http://hdl.handle.net/2433/128959>

RIGHT:

© 2010 Elsevier Ltd; この論文は出版社版ではありません。引用の際には出版社版をご確認ご利用ください。 ; This is not the published version. Please cite only the published version.

Analysis of subthreshold photo-leakage current in ZnO thin-film transistors using indium-ion implantation

Yudai Kamada^{a,b,*}, Shizuo Fujita^a, Takahiro Hiramatsu^c, Tokiyoshi Matsuda^c, Mamoru Furuta^c, and Takashi Hirao^c

^aDepartment of Electronic Science and Engineering, Kyoto University,
Katsura, Nishikyo-Ku, Kyoto 615-8510, Japan

^bPhotonics and Electronics Science and Engineering Center, Kyoto University
Rohm Plaza, Katsura, Nishikyo-ku, Kyoto 615-8520, Japan

^cResearch Institute for Nanodevices, Kochi University of Technology,
185, Miyanokuchi, Tosayamada-cho, Kami, Kochi 782-8502, Japan

Abstract

Mechanism of photo-leakage current in the ZnO TFTs has been analyzed by comparison between the light irradiated TFTs and indium (In) ion implanted TFTs where the selected areas of the channel region were irradiated or implanted. In case of the TFT with In ion implantation at a source region, the positive charge of ionized donors at the source region lowered the potential barrier at the source electrode and increased leakage current even at a dark condition due to carrier injection from the source into the channel region. In case of light irradiation of the ZnO TFT, similar phenomenon was observed due to the hole accumulation at the source region. From the analogy of the leakage properties, it is confirmed that the photo-leakage current is mainly due to the accumulation of holes near the source electrode, which lowers the potential barrier for the carrier injection from the source to the channel region, contributing to the generation of the leakage current.

Keywords : ZnO; Photosensitivity; Implantation

*Corresponding author. E-mail address : kamada@icc.kyoto-u.ac.jp

1. Introduction

Transparent oxide-based thin-film transistors (TFTs) attract a great deal of interest for transparent electronics not only for display applications [1-3] but also as stacked image sensors [4], electronic papers [5] and transparent electronic circuits [6]. Transparency in the visible light is a remarkable advantage of wide-gap oxide semiconductors, not shared by conventional silicon based materials. Nevertheless large photo-leakage current induced even by below-band-gap light in oxide TFTs limits many practical applications [7-10]. Figure 1 shows transfer characteristics of a ZnO TFT with a drain voltage (V_d) of 10 V under dark and light irradiation. Photon energy at a wavelength of 370 nm corresponds approximately to the band gap energy of ZnO thin films used in this experiment. The intensity of the light was maintained at $200 \mu\text{W}/\text{cm}^2$. As shown in Fig. 1, the off-state leakage current of the ZnO TFT was significantly increased even at a blue-light (400 nm) irradiation. This photosensitivity in the visible light is a fatal for transparent electronics applications.

On the basis of experimental results of irradiation-position dependence in ZnO TFTs, we previously reported that the photo irradiation at source region is most sensitive to the photo-leakage current [11], resulting in an adverse effect on the transparency in the visible light. From the results, we proposed that major element of photo-leakage current is the potential modulation in the source region due to the hole accumulation, resulting in increasing the carrier injection from the source into the channel region. In this paper, the mechanism of photo-leakage current in the ZnO TFTs have been analyzed by using indium (In) ion implantation. In ions were implanted into the selected area only at source or drain region of

ZnO channel. From the comparison of the leakage current between the un-implanted TFTs under light irradiation and the In implanted TFTs under dark condition, we propose the mechanism of the photo-leakage current in the ZnO TFTs.

2. Photo-leakage current in ZnO TFTs

In order to compare the photo-leakage current characteristics under the source-side irradiation and the drain-side irradiation, the ZnO TFT samples as shown in Fig. 2 (a) and (b) were prepared. The fabrication process of the ZnO TFTs was reported previously [11, 12]. The ZnO film used in this study was deposited on a $\text{SiO}_x/\text{SiN}_x$ (50/100 nm) gate insulator layer at 150 °C by a radio frequency (RF) magnetron sputtering. The detailed deposited conditions and the optical property of the ZnO film were also reported in the previous papers [11, 12]. In this study, the light shield layers of Cr metal were formed on the TFT in order to control the irradiation position of the incident light. The drain-side shielded TFT allows the irradiation at the half of the channel region from the source electrode, and the source-side shielded TFT allow that at the half of the channel region from the drain electrode.

Figure 3 shows the transfer characteristics of (a) the source-side irradiated TFT and (b) the drain-side irradiated TFT under various light intensities. Wavelengths of the light were 400 and 370 nm which consist of below and above the band gap energy of the ZnO film, respectively. Width to Length ratio of the TFT was 2.5 ($W/L = 50/20 \mu\text{m}$). The drain voltage was set at 10 V. The source-side irradiated TFTs exhibited large photosensitivity as compared with the drain-side irradiated TFTs, especially in the subthreshold region. The leakage current

was apparently induced by the photo irradiation because the leakage current monotonically increased as the irradiated light intensity increased.

Figures 4 and 5 depict the comparison of the transfer characteristics of the ZnO TFTs under source-side irradiation, drain-side irradiation, and dark condition. Irradiated wavelength of 400 nm and 370 nm were shown in Figs. 4 and 5 with an intensity of $200 \mu\text{W}/\text{cm}^2$. The drain voltage were (a) 0.1 V, (b) 2 V, (c) 5 V, and (d) 10 V. For the source-side irradiated TFTs, hump characteristics were observed in the subthreshold region when the drain voltage was higher than 2 V. In contrast, distinct hump characteristics were not observed in the drain-side irradiated TFTs. The degradation of subthreshold swing under drain-side irradiation is due to photo current [11] and the appearance of characteristic changes is obviously different as compared with those under source-side irradiation. These features are same under light irradiation below or above band gap energy as shown in Figs. 4 and 5. From the above results, it is obvious that the photosensitivity in the source region causes most harmful influence on the transparent properties in the visible light. As the mechanism for the phenomena, especially hump characteristics in the subthreshold region, we proposed the potential barrier lowering at the source electrode which enhanced carrier injection from the source to the channel region [11]. In proposed mechanism, the generation of leakage current is closely related to the conductivity distribution along the channel direction, therefore, the detailed analyses are required to reveal the generation mechanism of leakage current in ZnO TFTs.

3. Properties of indium ion implanted TFTs

In order to investigate the effect of partially modulation of the conductivity within the ZnO channel on the leakage current, the conductivity of the channel was partially modulated by In ion implantation. Matsuda et al. reported that the conductivity of ZnO thin film could be controlled by In ion implantation [13].

Indium ions, therefore, were selectively implanted either in the source side or in the drain side of the ZnO channel layer. These TFTs should replicate the transfer characteristics under the source-side irradiation and the drain-side irradiation even at a dark condition. Figure 6 depicts the key steps in the fabrication processes of the indium-implanted ZnO TFTs. First, a 50-nm-thick chromium film was patterned into gate electrode on a nonalkaline glass substrate, and a $\text{SiO}_x/\text{SiN}_x$ stacked film was continuously deposited as a gate insulators by conventional plasma-enhanced chemical vapor deposition (PECVD) at 350 °C (Fig. 6 (a)). Next, a 40-nm-thick ZnO for channel layer was deposited, followed by formation of a 25-nm-thick SiN_x as a protecting layer of the back channel surface. In order to obtain the steady TFT characteristics, thermal annealing of 375 °C was conducted for 3 h in a nitrogen atmosphere. Then, In ions were implanted into the ZnO channel through the SiN_x protecting layer with a dosage of $1 \times 10^{14} \text{ cm}^{-2}$ at an acceleration energy of 120 keV. The carrier density in the implanted region is evaluated to be as high as $1.3 \times 10^{19} \text{ cm}^{-3}$ from Hall measurement of the film prepared by similar thermal process to TFT fabrication, which is much higher as compared with un-implanted ZnO films used in the TFTs. Patterned photoresist was used as an implantation mask (Fig. 6 (b)). Two types of TFTs, which have different implanted regions, were prepared, that is, those where the In ions were implanted either in the source side or in

the drain side from the middle of the channel region. In this paper, these samples were named as a source-side implanted TFT and a drain-side implanted TFT, respectively. An un-implanted TFT was used as a control TFT. After the In ion implantation, the bilayer of ZnO and SiN_x was patterned into each TFT by a dry etching process. A 200-nm-thick SiN_x was then deposited as a interlayer insulator (Fig. 6 (c)). Finally, 50-nm-thick indium-tin-oxide (ITO) source/drain electrodes and 200-nm-thick SiN_x passivation layer were formed. (Fig.6 (d)).

Figure 7 shows the comparison of the transfer characteristics of the source-side implanted and the drain-side implanted TFTs at the different drain voltages of (a) 0.1, (b) 2, (c) 5, and (d) 10 V. The un-implanted TFTs (control TFTs) are shown in the Fig. 7 as a reference. It was confirmed that the source-side implanted TFT showed the hump characteristics in the subthreshold region even at the dark condition as compared with the control TFT when the drain voltage was higher than 2 V. Similar properties were observed in control TFTs under source-side irradiation as shown in Figs. 4 and 5. In contrast, the drain-side implanted TFT remains almost unchanged as compared to the control TFT.

Comparing Figs. 4 and 7, it is obvious that the source-side implanted TFT really replicates the transfer characteristics of the source-side irradiated TFT. In the off state, the amount of carrier injection from the source electrode to the channel region is limited by the potential barrier, which is normally controlled by negative gate voltage. Figure 8 illustrates conceptual diagram of generating leakage current in the subthreshold region (a) under light irradiation and/or of the indium implanted TFTs, (b) the corresponding schematic diagram of potential

modulation and (c) magnified view of potential distribution at the source region under various applied drain voltage. When In ions were implanted into the source region, numerous ionized donors influence on the potential distribution at the source region due to their positive charges. On the contrary, light irradiation induces numerous electron-hole pairs. The hole mobility in ZnO is much lower than the electron mobility [14] and the generated holes can be seen like immobile positive charges. In addition, it is predicted that the negative gate voltage assists the accumulation of hole at the ZnO/gate insulator interface. As the result, light-induced holes are thought to act just like ionized donors. The existence of these positive charges reduced potential barrier at the source electrode and enhanced carrier injection from the source to the channel region, contributing to the generation of the leakage current. Lateral electric field induced by drain voltage can also enhance the carrier injection because the potential barrier at the source electrode becomes lower as shown in Fig. 8 (c). On the other hand, the drain-side implanted TFT did not show remarkable change in transfer characteristics. This means that the potential modulation at the drain region does not influence the leakage current. The leakage current induced by photo irradiation (370 nm) on the drain region can be explained as photo current not by carrier injection.

In our proposed mechanism, photo-leakage current in the subthreshold region is mainly due to the potential barrier lowering at the source electrode by accumulated hole. Therefore, controlling the potential distribution along the channel direction will be useful for suppressing the photo-leakage current.

4. Conclusions

Mechanism of photo-leakage current in the ZnO TFTs has been analyzed by using In ion implantation. In ions were implanted into the selected area of the ZnO channel. In case of the photo irradiation, the source-side irradiated TFTs exhibited large photosensitivity as compared with the drain-side irradiated TFTs, especially in the subthreshold region. It is demonstrated that the similar phenomena of the leakage current was observed in the ZnO TFTs which were selectively implanted by In ions into only the source or drain regions. The implanted In ions are to generate positively ionized donors and to increase the conductivity partially. The existence of these positive charges contributes to reduce potential barrier at the source electrode and to enhance carrier injection from the source to the channel region. In case of the light irradiation in the ZnO TFTs, the hole mobility in ZnO is much lower than the electron mobility and the generated holes can be seen like immobile positive charges. In addition, negative gate voltage assists the accumulation of hole at the ZnO/gate insulator interface. From the results, therefore, photo-leakage current in the subthreshold region is also due to the potential barrier lowering at the source electrode by accumulated hole, mainly. The results obtained here are quite useful to find a clue for the control policies taken to suppress the leakage current of ZnO TFTs for transparent applications.

Acknowledgments

This work was partially supported by a Grant-in-Aid for Scientific Research from the Japan Society for the Promotion of Science and by the Global Center of Excellence program of the

Ministry of Education, Culture, Sports, Science and Technology.

References

- [1] Jeong JK, Jeong JH, Yang HW, Ahn TK, Kim M, Kim KS, et al. J. 12.1-in. WXGA AMOLED display driven by InGaZnO thin-film transistors. Soc. Inf. Disp. 2009;17(2);95-100.
- [2] Lee HN, Kyung J, Sung MC, Kim DY, Kang SK, Kim SJ, et al. Oxide TFT with multiplayer gate insulator for backplane of AMOLED device. J. Soc. Inf. Disp. 2008;16(2);265-72.
- [3] Hirao T, Furuta M, Furuta H, Matsuda T, Hiramatsu T, Hokari H, et al. Novel top-gate zinc oxide thin-film transistors (ZnO TFTs) for AMLCDs. J. Soc. Info. Disp. 2007;15(1);17-22.
- [4] Aihara S, Seo H, Namba M, Watabe T, Ohtake H, Kubota M, et al. Stacked Image Sensor With Green- and Red-Sensitive Organic Photoconductive Films Applying Zinc Oxide Thin-Film Transistors to a Signal Readout Circui. IEEE trans Electron Devices 2009;56(11);2570-76.
- [5] Ito M, Miyazaki C, Ishizaki M, Kon M, Ikeda N, Okubo R, et al. Application of amorphous oxide TFT to electrophoretic display. J.Non-cryst.Solids, 2008;354;2777-82.
- [6] Hayashi R, Ofuji M, Kaji N, Takahashi K, Abe K, Yabuta H, et al. Circuits using uniform TFTs based on amorphous In-Ga-Zn-O. J. Soc. Info. Disp. 2007;15(11);915-21.
- [7] Takechi K, Nakata M, Eguchi T, Yamaguchi H, Kaneko S. Comparison of Ultraviolet Photo-Field Effects between Hydrogenated Amorphous Silicon and Amorphous InGaZnO₄ Thin-Film Transistors. Jpn. J. Appl. Phys. 2009;48;010203.
- [8] Jeon K, Kim C, Song I, Park J, Kim S, Kim S, et al. Modeling of amorphous InGaZnO thin-film transistors based on the density of states extracted from the optical response of capacitance-voltage characteristics. Appl.Phys.Lett. 2008;93;182102.
- [9] Cho J, Jeong J, Lee HN, Kim HG, Kim ST, Hong Y. Instability Behavior of Oxide-based Top-gate TFTs under Electrical and Optical Stress Test. ESC transactions. 2008;16(9);115
- [10] Gosain DP, Tanaka T. Instability of Amorphous Indium Gallium Zinc Oxide Thin Film Transistors under Light Illumination. Jpn. J. Appl. Phys. 2009;48;03B018.
- [11] Kamada Y, Fujita S, Hiramatsu T, Matsuda T, Nitta H, Furuta M, et al. Photo-Leakage

Current of Zinc Oxide Thin-Film Transistors. Jpn. J. Appl. Phys. 2010;49;03CB03.

[12] Hirao T, Furuta M, Hiramatsu T, Matsuda T, Li C, Furuta H, et al. Bottom-Gate Zinc Oxide Thin-Film Transistors (ZnO TFTs) for AM-LCDs. IEEE Trans Electron Devices. 2008;55(11);3136-42.

[13] Matsuda T, Furuta M, Hiramatsu T, Furuta H, Hirao T. Crystallinity and resistivity of ZnO thin films with indium implantation and postannealing. J. Vac. Sci. Technol. A. 2010;28(1);135-38.

[14] Ogo Y, Hiramatsu H, Nomura K, Yanagi H, Kamiya T, Hirano M, et al. p-channel thin-film transistor using p-type oxide semiconductor, SnO. Appl.Phys.Lett. 2008;93;032113.

Figure captions

Fig. 1 : Typical variation of drain current versus gate voltage transfer characteristics of a regular ZnO TFT against photo irradiation with different wavelengths.

Fig. 2 : ZnO TFT sample structures to discuss the difference in photosensitivity under (a) source-side irradiation and (b) drain-side irradiation.

Fig. 3 : Transfer characteristics of ZnO TFTs under (a) source-side irradiation and (b) drain-side irradiation with various light intensities.

Fig. 4 : Comparisons of transfer characteristics of ZnO TFTs under source-side irradiation, drain-side irradiation, and dark condition at the different drain voltages of (a) 0.1 V, (b) 2 V, (c) 5 V, and (d) 10 V. The irradiation wavelength was 400 nm. The red and solid lines are for the source-side irradiation, and the blue and dashed lines are for the drain-side irradiation. The characteristics under the dark condition are shown as black and solid lines.

Fig. 5 : Comparisons of transfer characteristics of ZnO TFTs under source-side irradiation, drain-side irradiation, and dark condition at the different drain voltages of (a) 0.1 V, (b) 2 V, (c) 5 V, and (d) 10 V. The irradiation wavelength was 370 nm. The red and solid lines are for the source-side irradiation, and the blue and dashed lines are for the drain-side irradiation. The characteristics under the dark condition are shown as black and solid lines.

Fig. 6 : Fabrication processes of indium-implanted ZnO TFTs.

Fig. 7 : Comparisons of transfer characteristics of source-side indium-implanted, drain-side indium-implanted, and un-implanted ZnO TFTs at the different drain voltages of (a) 0.1 V, (b) 2 V, (c) 5 V, and (d) 10 V. The red and solid lines are for the source-side implanted TFT and the blue and dashed lines are for the drain-side implanted TFT. The characteristics of un-implanted TFT are shown as black and solid lines.

Fig. 8 : Conceptual diagram of generating leakage current in the subthreshold region (a) under light irradiation and/or of the indium implanted TFTs, (b) the corresponding schematic diagram of potential modulation and (c) magnified view of potential distribution at the source region under various applied drain voltage.

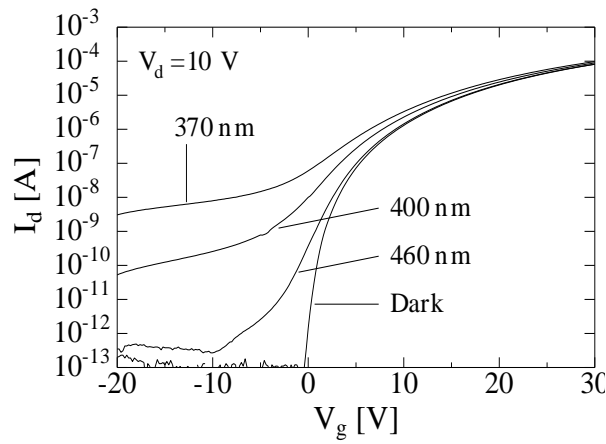


Figure.1

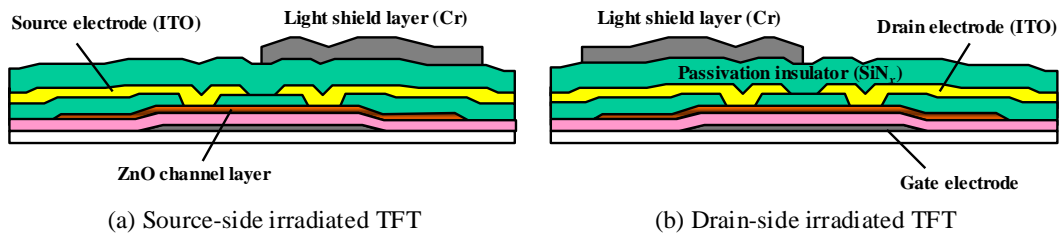


Figure. 2

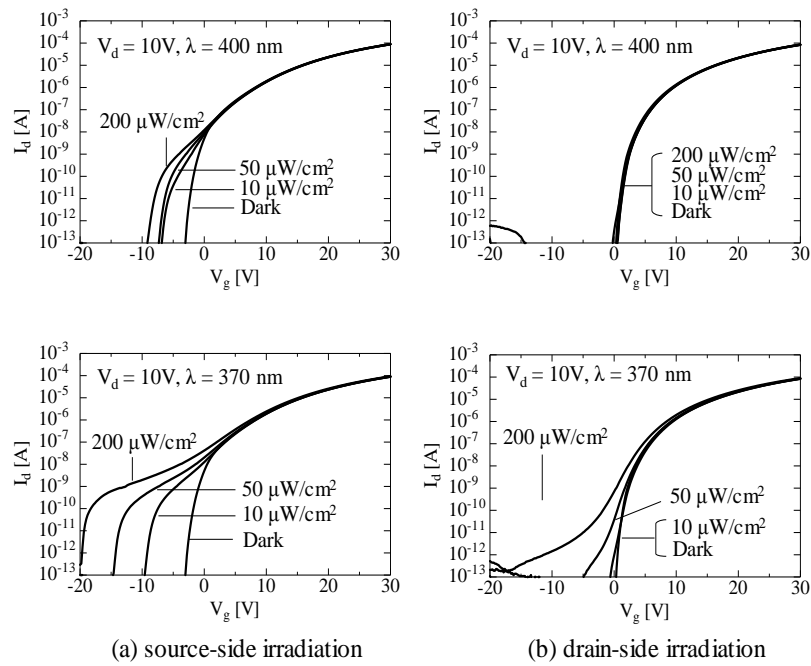


Figure.3

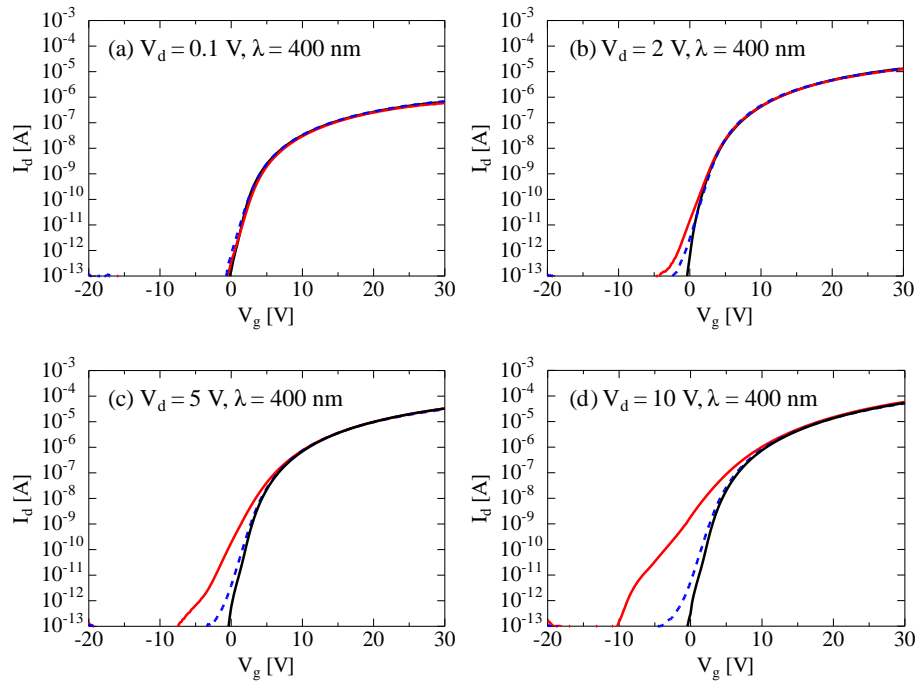


Figure.4

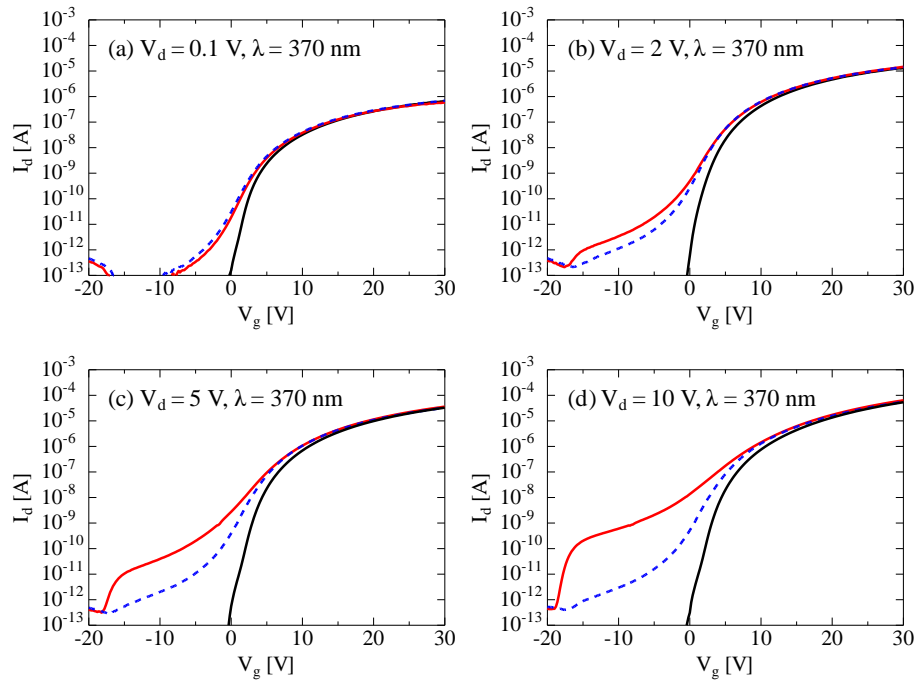


Figure.5

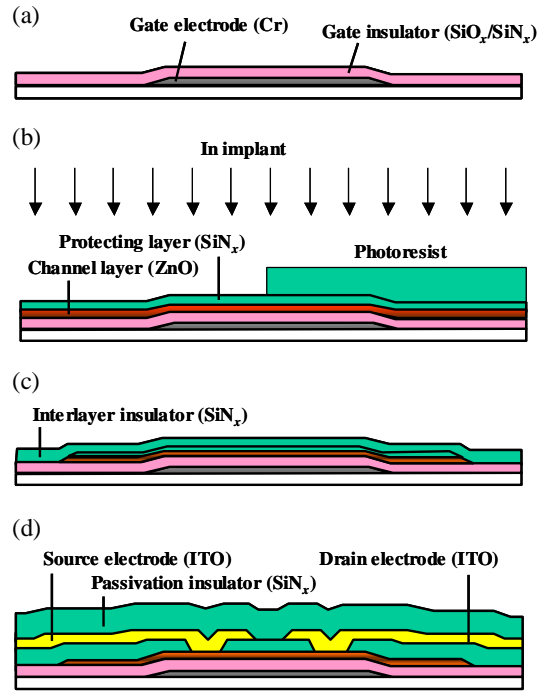


Figure.6

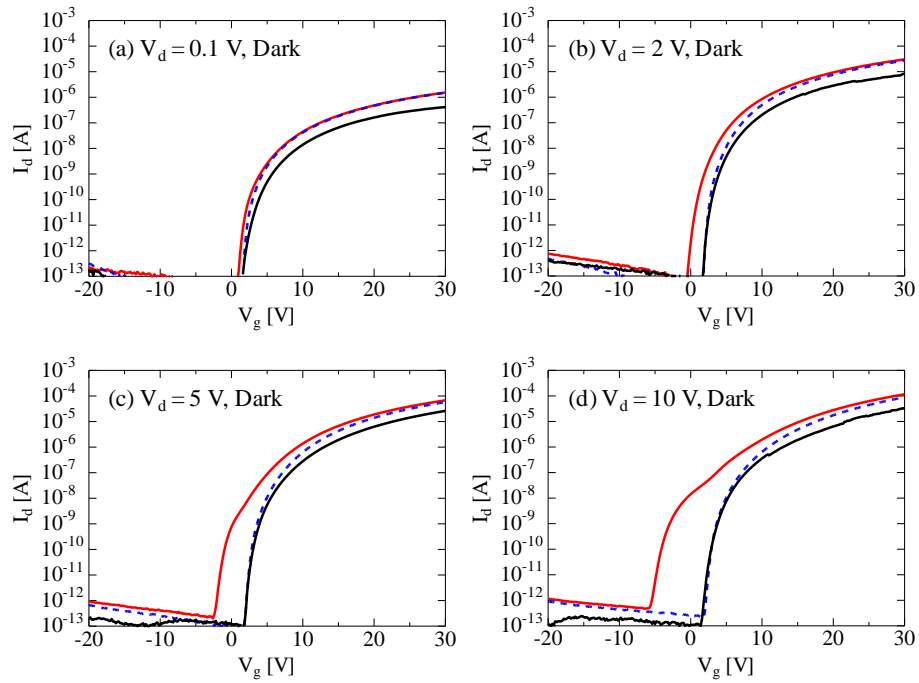


Figure.7

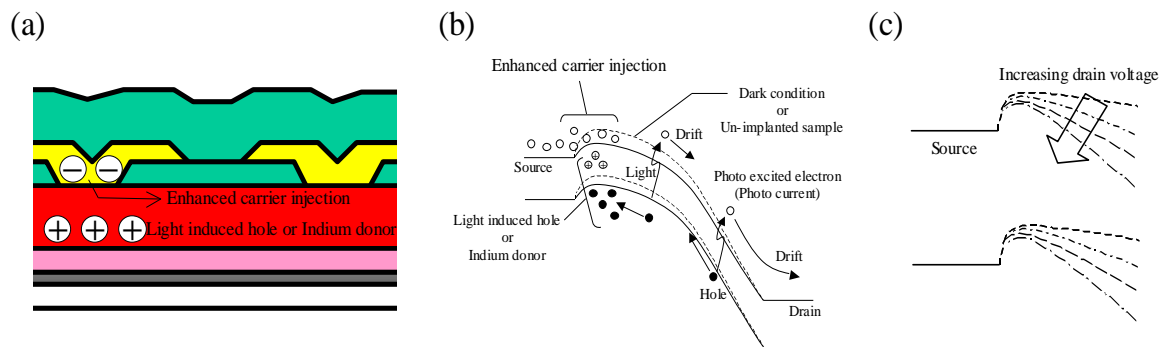


Figure. 8